Macromolecular Bioscience
www.mbs-journal.de

Effect of Core-Crosslinking on Protein Corona Formation on Polymeric Micelles

Irina Alberg, Stefan Kramer, Christian Leps, Stefan Tenzer, and Rudolf Zentel**

Most nanomaterials acquire a protein corona upon contact with biological fluids. The magnitude of this effect is strongly dependent both on surface and structure of the nanoparticle. To define the contribution of the internal nanoparticle structure, protein corona formation of block copolymer micelles with poly(*N*-2-hydroxypropylmethacrylamide) (pHPMA) as hydrophilic shell, which are crosslinked—or not—in the hydrophobic core is comparatively analyzed. Both types of micelles are incubated with human blood plasma and separated by asymmetrical flow field-flow fractionation (AF4). Their size is determined by dynamic light scattering and proteins within the micellar fraction are characterized by gel electrophoresis and quantified by liquid chromatography-high-resolution mass spectrometry-based label-free quantitative proteomics. The analyses reveal only very low amounts of plasma proteins associated with the micelles. Notably, no significant enrichment of plasma proteins is detectable for core-crosslinked micelles, while noncrosslinked micelles show a significant enrichment of plasma proteins, indicative of protein corona formation. The results indicate that preventing the reorganization of micelles (equilibrium with unimers) by core-crosslinking is crucial to reduce the interaction with plasma proteins.

1. Introduction

The field of nanomedicine has emerged worldwide. Therefore, various types of nanocarriers were developed in order to deliver a specific cargo to the desired site. Most of the nanocarriers share a common feature, the formation of a core–shell structure by a self-assembly process. The core can be employed to encapsulate drugs and is often used to crosslink the architecture and thereby stabilize it, so disassembly due to dilution cannot occur.[1] The outer shell and surface of the nanocarrier is hydrophilic and has a protective function. A perfect shell material should prevent nonspecific interactions and should ideally show no interactions with proteins or other blood components, since the adsorption of proteins can lead to aggregation, can hide recognition units or can cause early clearance of the nanocarrier.[2–7]

As of today, several polymeric micelles are in advanced stages of clinical testing or even approved by the food and drug administration for nanomedical applications.[8–10] One example is CPC634, core-crosslinked micelles with covalently bound docetaxel, which are in clinical phase II and have nicely demonstrated the complete regression of breast tumors by a single injection in mice.[11,12] The more and more widespread use of micelles in the field of nanomedicine may result from the fact that especially micelles seem to have reduced interactions with proteins and are stable in plasma, which is a requirement for a successful application as drug delivery system.[13–18]

When nanoparticles are administered intravenously into the body, their first contact is with plasma proteins in the blood. This interaction can lead to the formation of a protein corona. Thus, to get an indication of the stability of nanoparticles in the body, the formation of a protein corona on nanocarriers has been a major focus of nanomaterial research. Thereby, protein corona formation in contact with blood plasma was observed for many systems.[3,19–24] And since such a corona changes the identity of the particle and modifies its fate in the body, its characterization is very important for drug delivery systems.[7,25–28] Throughout all the nanoparticles, which were characterized regarding pronounced protein corona formation, most were colloids or "hard" nanoparticles with a sharp hydrophobic and/or charged surface.[18,29–31] For these types of nanoparticles, this interphase dominates the interaction with plasma proteins.[17,18,32–34] For example, polystyrene nanoparticles typically acquire a thick and tightly bound protein layer around the nanoparticle, which is also termed "hard protein corona."[35–37] This happens because a sharp and distinct surface can induce a change of the conformation (denaturation) of plasma proteins[38] in order to increase the interactions with the hydrophobic and charged

Dr. I. Alberg, Dr. S. Kramer, Prof. R. Zentel
Department of Chemistry
Johannes Gutenberg University Mainz
Duesbergweg 10-14, 55099 Mainz, Germany
E-mail: zentel@uni-mainz.de

C. Leps, Prof. S. Tenzer
Institute for Immunology
University Medical Center of Mainz
Langenbeckstr. 1, 55131 Mainz, Germany
E-mail: tenzer@uni-mainz.de

The ORCID identification number(s) for the author(s) of this article can be found under https://doi.org/10.1002/mabi.202000414.

DOI: 10.1002/mabi.202000414

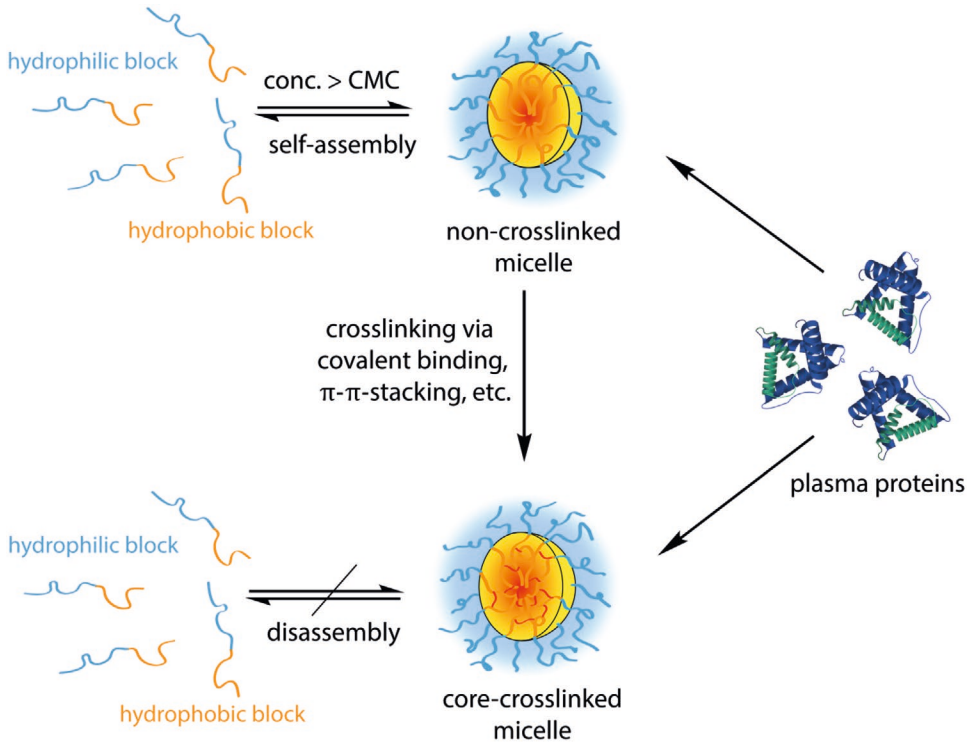

Figure 1. Illustration of the self-assembly and crosslinking process of amphiphilic block copolymers. Do noncrosslinked and core crosslinked micelles interact differently with plasma proteins?

surface. The denaturation of the proteins can in turn trigger further interactions with proteins.[38]

In this context, it is important that protein adsorption on hard and macroscopic surfaces can be strongly reduced or even eliminated by grafting the surface densely with rather hydrophilic, strongly hydrated polymers, which are selected according to the so-called "Whitesides rules."[34] They prevent the contact of the surface with plasma proteins by purely entropic forces. Polymeric micelles follow the same rule. They are composed of amphiphilic block copolymers, which self-assemble into organized structures in water (**Figure 1**). In this structure the hydrophobic core (consisting of the hydrophobic blocks) is densely coated with the water soluble blocks. Due to this structure protein corona formation can thus be very small or even below detection limits,[17] as proven for some crosslinked micellar structures.

The situation for (noncrosslinked) micelles or colloids is, however, more complex because of kinetic reasons. Here, it is interesting to consider work on colloids from polystyrene (PS), which are stabilized with various (also PEGylated) detergents.[18,39–41] In this case, the surface will—on average—also be coated with hydrophilic polymers (PEG), but due to the dynamic exchange of the detergents (unimers in equilibrium with micelles, critical micelle concentration, CMC), parts of the hydrophobic surface will also get constantly accessible to proteins under equilibrium conditions as discussed in [18]. An extensive corona formation from plasma proteins would be the result in this case.[35–37] Thus, to avoid such corona formation, it is highly important to prevent a rearrangement of the surface structure. This situation may also apply to polymeric micelles, because also self-assembled nanocarriers from block copolymers disassemble in equilibrium—due to their dynamic nature—partly into unimers. This can also be seen by the elimination of radioactively labeled block copolymer micelles with low CMC via the kidneys although the micelles—by themselves—are much too large for kidney passage (polymer **P0**% in ref. [30] is thereby very similar to the noncrosslinked block copolymer studied here).[30,42] Here, crosslinking of the self-assembled micellar structure is the key to stabilize the nanocarrier in the body in order to avoid rearrangement, aggregation, and clearance by the kidney.[1,30,43] To achieve this, the individual polymers of the self-assembled structures have to be covalently linked (or stabilized by strong noncovalent interactions), so that the dynamic of the nanoparticle is "frozen." As a result after crosslinking, the nanoparticular structure represents one large single molecule and is protected against dissociation (Figure 1) . However, it is—so far—not clear whether a stabilization of the structure of the nanocarrier concerning the interaction with plasma proteins is really necessary.

Recently, we established a new method for the characterization of the protein corona of various polymeric nanocarriers by using asymmetrical flow-field flow fractionation (AF4) combined with label-free liquid chromatography-high-resolution mass spectrometry (LC-MS).[17] To investigate the effect of crosslinking (prevention of the rearrangement of the micellar structure) on the interaction with plasma proteins, we here apply this method to characterize the protein corona of noncrosslinked and core-crosslinked micelles, which are based on poly(*N*-2-hydroxypropylmethacrylamide) (pHPMA) block copolymers.[29]

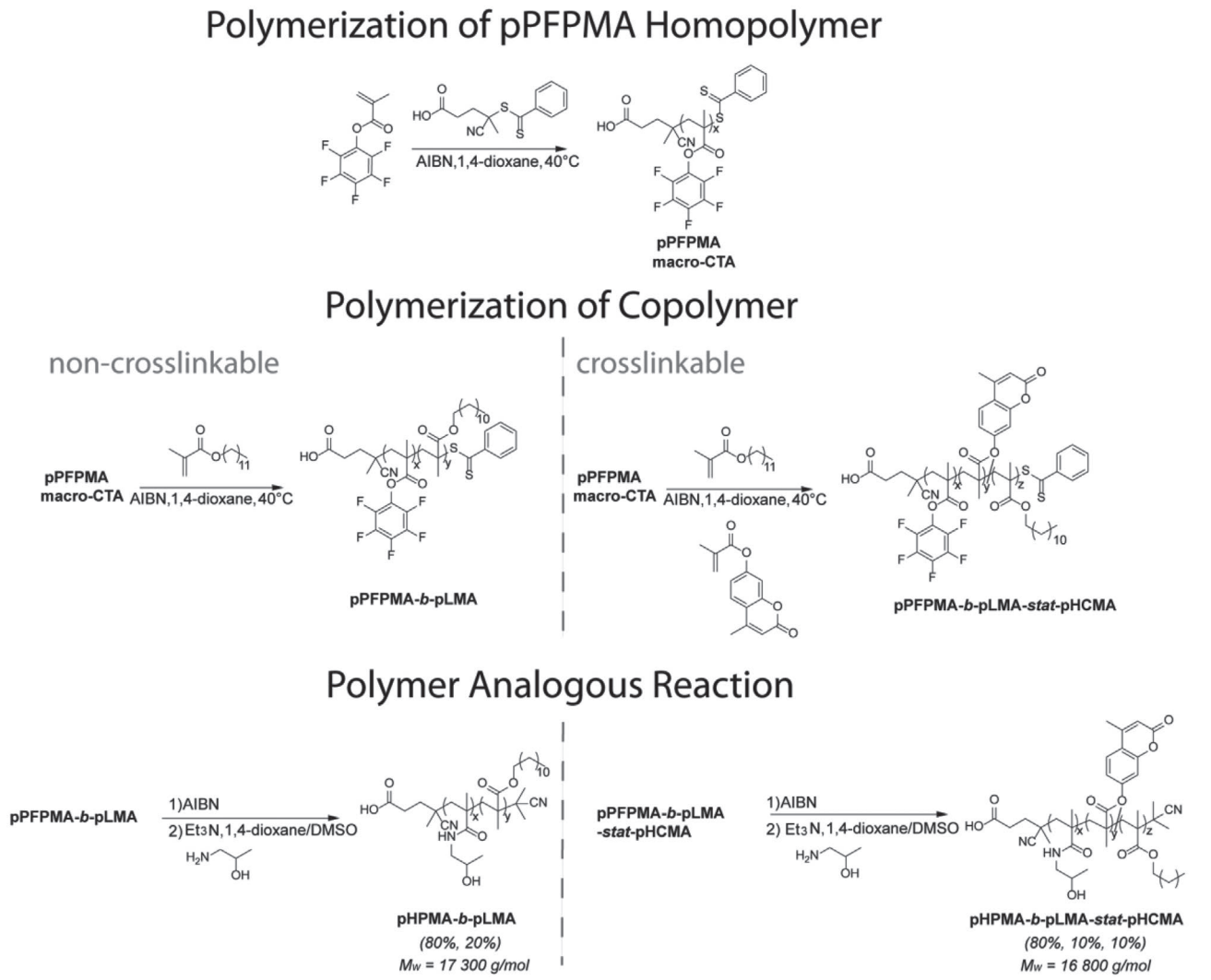

Figure 2. Synthetical pathways for the amphiphilic block copolymers (pHPMA-b-pLMA-stat-pHCMA) and (pHPMA-b-pLMA).

2. Results and Discussion

To enable the comparative analysis of corona formation between crosslinked and noncrosslinked systems on otherwise nearly identical nanocarriers, we prepared pHPMA-based micelles from poly(N-(2-hydroxypropyl) methacrylamide)-*b*-poly(lauryl methacrylate) (pHPMA-*b*-pLMA) or poly(*N*-(2-hydroxypropyl) methacrylamide)-*b*-poly(lauryl methacrylate-*stat*-hymecromone methacrylate) (pHPMA-*b*-pLMA-*stat*-pHCMA) block copolymers by solvent switching as described recently.[29] These systems closely resemble each other except that the micelles consisting of the (pHPMA-*b*-pLMA-*stat*-pHCMA) block copolymers can be crosslinked by a [2+2] cycloaddition of the hymecromone unit.[29]

The synthesis, chemical structure, and composition of the block copolymers is illustrated in **Figure 2** and is fully described.[29] Briefly, after the RAFT (reversible addition fragmentation chain-transfer) polymerization of the reactive ester monomer pentafluorophenyl-methacrylate (PFPMA) with the chain transfer agent (CTA) 4-cyano-4-(phenylcarbonothioylthio)-pentanoic acid, the resulting poly PFPMA (pPFPMA) homopolymer is used as a macro-CTA to copolymerize either laurylmethacrylate (LMA) or both LMA and hymecromone methacrylate (HCMA) to achieve block copolymers with an additional crosslinking unit. Subsequent to the removal of the reactive dithiobenzoate end group, the block copolymers are converted into amphiphilic block copolymers by aminolysis of the pPFPMA block with 2-hydroxypropylamine (HPA). The achieved block copolymers were used to form core-crosslinked and noncrosslinked micelles with comparable size (**Table 1**). For more details regarding polydispersity index and the about neutral zeta potential see the Supporting Information section (Table S1, Supporting Information).

We chose thereby these polymers, as polymers from pHPMA are well characterized[44] and used as carriers for a long time.[13,45–48] In addition, the block copolymers used here are known to have very little unspecific cellular uptake[49] and they can be easily modified for immune cell activation.[50] Their properties have been summarized recently.[44] The CMC of block copolymers of similar composition was found to be in

Table 1. Comparison of the hydrodynamic radii for core-crosslinked and noncrosslinked pHPMA-based micelles after separation in AF4 and incubation in different solutions.

Nanoparticle	R_h upon incubation in PBS [nm][a)]	R_h upon incubation in plasma [nm][a)]
pHPMA micelles crosslinked	19.4	18.2
pHPMA micelles noncrosslinked	17.3	17.6

[a)]DLS measurements for noncrosslinked micelles were performed by a Malvern Zetasizer.

the low range of 10^{-5} and 10^{-4} mg mL^{-1}.[30,44,49] Besides, pHPMA homopolymers of 65 kDa display a blood half-life of 10 h.[51] Thus, generally, surface coating with pHPMA reduces protein adsorption.[52]

Concerning the comparison of crosslinked and noncrosslinked structures, it should thereby be considered that the difference is not a priori clear. On the one hand, a planned crosslinking reaction may not be as successful as intended, because the effect of crosslinking may be smaller than expected. Alternatively, the mobility within the hydrophobic core may be already very small, even in the absence of crosslinking.

On the other hand, although the crosslinkable unit in the polymeric micelles is mostly located in the inner core (core-crosslinking), which requires it to be hydrophobic itself, it may still be in contact with the aqueous medium. If parts of the hydrophobic crosslinking structure would be exposed to the outer surface of the micelle, proteins are likely to interact with it, resulting in corona formation. This effect can, however, not be too strong, as the core-crosslinked, pHPMA-based micelles were already characterized in a recent study, where the protein corona was determined to be neglectable, since most of the particles were not associated with a single protein.[17]

After preparation of the noncrosslinked micellar system, we applied our AF4-based separation method, as described recently,[17] in order to separate the nanoparticles from the protein incubation solution for further analysis of the NP-protein-complex. AF4 is a chromatography-like separation technique based on differences in the hydrodynamic radii of the species which should be separated.[53] We chose AF4 as separation method, since the contact of the separated sample with the membrane is minimal (or ideally not existing) and the separation conditions are very mild due to the strongly reduced shear forces.[54–57] **Figure 3** shows the AF4 elugrams of both types of incubated pHPMA-based micellar systems and the respective control runs. In both elugrams (crosslinked and not crosslinked), the run from the pure micelles is illustrated in green, the run from pure plasma in red and the run from the mixture between micelles and plasma in blue. The initial, intense peak between 7 and 12 min can be assigned to smaller proteins from the plasma. The second peak, which appears at 12.5 or 15 min (depending on the size of the micelles and the crossflow of the measurement), represents the eluting micelles. The third peak in both elugramms is caused by plasma eluted after reducing the gradient cross flow from the high initial flow rate to a flow rate of 0 mL min^{-1}. It is not part of the separation itself. Generally, a high cross flow leads to broadened elution

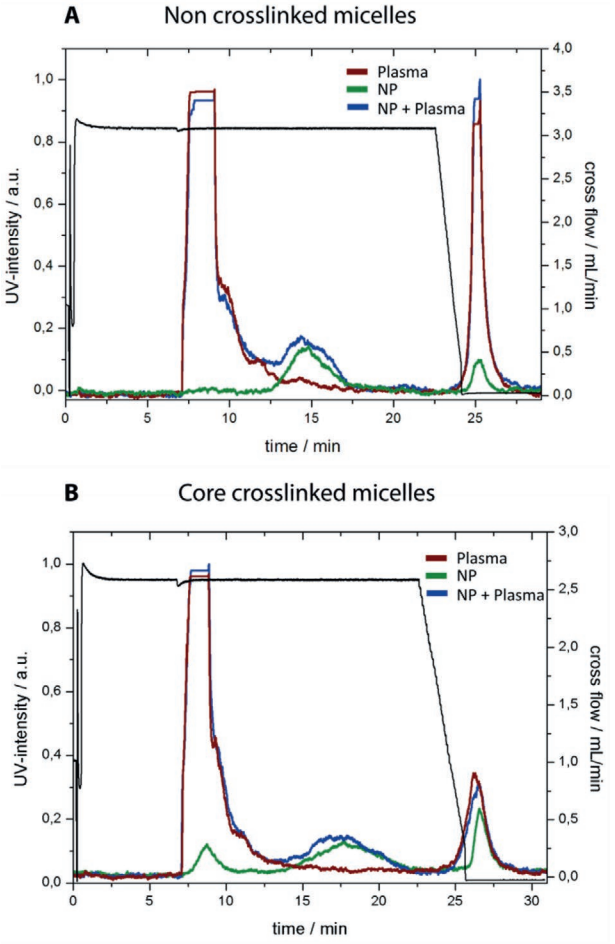

Figure 3. AF4 elugrams of A) core-crosslinked pHPMA micelles and B) noncrosslinked pHPMA micelles. NPs (green), plasma (red), and in plasma incubated NPs (blue). UV detector at 220 nm.

peaks and to longer retention of both the NP and the plasma proteins in AF4. The starting flow rate in Figure 3A is higher than in Figure 3B. Thus, the second plasma peak is higher in this case, since more of the proteins are retained at the beginning.

Independent of these details it is evident that the noncrosslinked micelles (Figure 3A) can be well separated from the plasma proteins and they retain their size after incubation with plasma. Their behavior is, thus, in good agreement with that of the core-crosslinked pHPMA micelles (Figure 3B). This indicates that the protein adsorption is, also for the noncrosslinked micelles, rather low and the size of the micelles is not changed by protein adsorption. Additionally, the unaltered size could be confirmed by dynamic light scattering (DLS) experiments (Table 1).

In order to identify potentially adsorbed proteins, we performed sodium dodecyl sulfate polyacrylamide gel electrophoresis (SDS-PAGE) of the noncrosslinked micelles followed by silver staining, which is presented in **Figure 4** (SDS-PAGE) of core-crosslinked micelles can be seen in Figure S1, Supporting Information). As in the case of the core-crosslinked micelles, no proteins were detectable by Coomassie staining in the recovered noncrosslinked micelles. Only the very sensitive silver

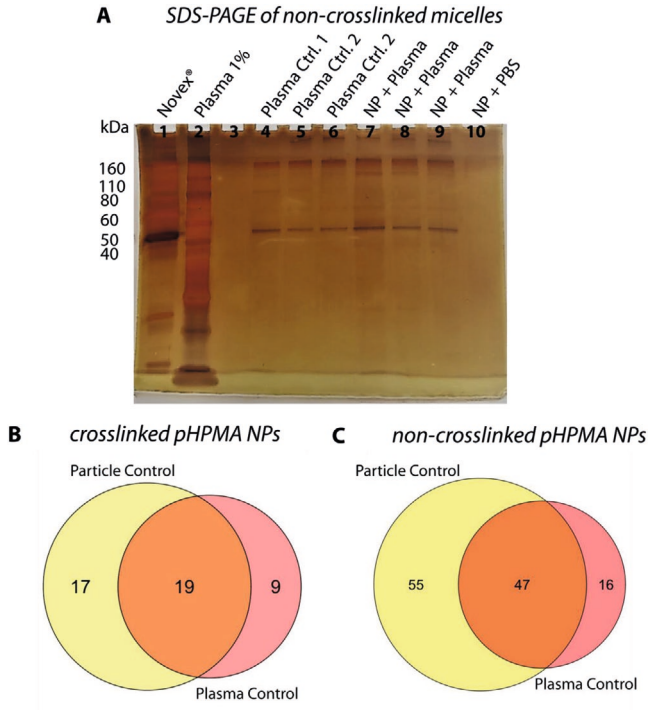

Figure 4. A) Silver stained SDS-PAGE gel of AF4 fractions from three independent measurements of noncrosslinked pHPMA micelles. 1) Novex Sharp prestained protein standard, 2) Human blood plasma 1%, 3) Empty, 4) Plasma + PBS (plasma control 1), 5) Plasma + PBS (plasma control 2), 6) Plasma + PBS (plasma control 3), 7) NP + Plasma from AF4 (1), 8) NP + Plasma from AF4 (2), 9) NP + Plasma from AF4 (3), 10) NP + PBS (particle control). B,C) Venn-Diagrams for enriched proteins on pHPMA micelles. B) For crosslinked pHPMA micelles, C) for noncrosslinked pHPMA micelles. The overlap area shows the number of proteins significantly enriched (i.e., the protein corona) in the sample compared to both control conditions.

staining revealed traces of proteins. Figure 4 shows the silver stained SDS-PAGE gel obtained for the AF4 fractions from three independent experiments of the noncrosslinked micelles and the respective control runs. Thereby, as expected, no protein band is detected in the particle control (slot 10) because this sample was separated by AF4 after incubation in phosphate buffered saline (PBS), and thus was never in contact with plasma proteins. In the fractions from the plasma incubated micelles several protein bands could be detected (slot 7, 8, and 9), whereby one distinct band corresponds to human serum albumin (HSA, 67 kDa). HSA is the most abundant plasma protein and can be found in each (plasma included) AF4 run, since it is dragged within the AF4 channel. Hence, it is also detected in the plasma control runs (slot 4, 5, and 6), indicating that HSA is—at least in majority—simply coeluting and not adsorbed at the surface of the noncrosslinked micelles. In addition, several other proteins are also present in both the plasma control runs as well as in the fractions from the plasma incubated micelles. Thereby, the intensities of the bands resemble each other and cannot be assigned to higher protein amounts. At this point the situation of crosslinked and noncrosslinked micelles is very similar. There is—at least—very little corona formation and the collected proteins may all be coeluting. This demonstrates that crosslinking is not necessary to prevent the formation of a "prominent" protein corona for the pHPMA block copolymers studied here.

To look more into the details, we used the approach described recently[17] to characterize the corona of the micelles with more accuracy. By LC-MS we can determine small amounts of proteins and we consider them only as a part of the protein corona, if they are significantly enriched relative to both control conditions, namely the particle and the plasma control (Figure 4B,C). Therefore, we compare the collected AF4 fractions from the micelles (which were incubated in plasma and separated by AF4) to AF4 fractions from solution of pure plasma (plasma control) and of pure micelles (particle control). With this method, we found that from 118 regulated proteins (obtained after AF4 purification) only 47 were enriched relative to both controls and thus part of the protein corona of the noncrosslinked micelles (Table S2, Supporting Information). By this comparison it became also clear that most proteins detected by SDS-PAGE (most prominent human serum albumin, HSA) are not part of the protein corona, because they were found—at same concentrations—in the plasma control. That means they are simply coeluting. This means that the majority of the proteins detected by LC-MS were not part of the protein corona (**Figure 5**).

This must, however, be compared to only 19 enriched proteins detected for the crosslinked micelles. This indicates that the protein corona for the noncrosslinked system is not prominent, but more pronounced. Of the 47 corona proteins 18 of the noncrosslinked micelles were immunoglobulins, 6 were apolipoproteins (including clusterin), 4 were involved in the

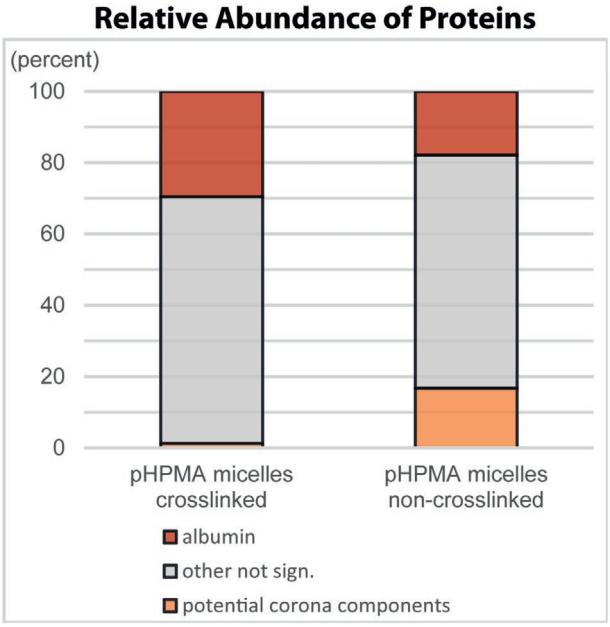

Figure 5. Relative abundance of proteins (percentage wise), detected in the AF4 fractions of the plasma incubated pHPMA micelles. Each bar represents the complete amount of protein detected in the sample shown as average across all biological and technical replicates. Red reflects the percentage share of HSA, gray all other proteins and orange shows the partition of the significantly enriched proteins (the protein corona).

coagulation cascade, and 8 were genuine factors of the complement system (Table S2, Supporting Information). In contrast, only 5 immunoglobulins, 2 apolipoproteins (including clusterin), and 1 protein involved in the complement system (as inhibitor) were part of the protein corona for the crosslinked micelles (Table S3, Supporting Information). This illustrates a huge difference in the corona composition.

Although some proteins were identical in between both micellar systems (immunoglobulin kappa variable 3D-20, haptoglobin-related protein, clusterin, serum amyloid P-component, serum amyloid A-4 protein, and plasma protease C1 inhibitor), the majority of the proteins found in the corona of the noncrosslinked micelles are immunoglobulins or proteins involved in the complement and coagulation cascade. Thus, this micellar system might by recognized by the immune system after exposure to plasma proteins, which is not the case for the crosslinked micelles. Since both systems possess the same chemical surface, this implies that the core of the noncrosslinked micelles is more accessible for protein interactions. This is in agreement with results by Elsabahy et al., who characterized the effect of crosslinking on interactions with biomolecules and toxicity.[31] Interestingly, a high amount of apolipoproteins could also be detected for the noncrosslinked systems. This suggests that unimers of the dynamic micellar system might interact via their hydrophobic blocks with highly hydrophobic proteins, such as apolipoproteins. In this respect, Li et al. demonstrated that noncrosslinked micelles can lose their assembly structure and release their payload upon interaction with lipoproteins.[58]Nevertheless, it should be mentioned, that the total amount of adsorbed proteins on the noncrosslinked micelles is—as in the case of the crosslinked micelles—still very low, since DLS analysis indicates that their size was not altered by the adsorbed proteins (Figure 3A; and Table S2, Supporting Information). This was, in addition, confirmed by proteomic analysis. Figure 5 shows the relative percentage of the significantly enriched proteins on both micellar systems. Thereby, only about 17% of the total amount of detected proteins on the noncrosslinked micelles consist of true corona proteins. However, this is still more than a tenfold increase of the enriched protein amount of the crosslinked micelles (1.3%). Thus, a distinct difference was found between both systems, whereby the crosslinked micelles seem to be less prone to protein adsorption. This highlights the significance of crosslinking when applying self-assembled systems in the field of nanomedicine, which was already pointed out by Talelli et al.[1]

Furthermore, it should be considered that the incubation conditions do not reflect the conditions in vivo, whereby a dynamic system has not only to struggle with high concentrations of proteins and other blood components, but also with dilution in the blood stream. As described recently here,[17] the core-crosslinked pHPMA micelles exhibit a remarkably prolonged circulation time of above 24 h, whereas Allmeroth et al.[30] showed a major kidney uptake and thus renal clearance from the body within a few hours for noncrosslinked pHPMA micelles, which resemble the system tested in this work. Hence, although the noncrosslinked micelles seem to be stable in plasma during in vitro experiments, they are rather not as suitable for nanomedical application by systemic administration due to their dynamic nature.

Associated with this observation is the question, if crosslinking has an influence on the transport of drugs with micellar systems. Now, to our knowledge there are no existing data to answer this question, but the—more general—aspect of the transport of hydrophobic drugs in the hydrophobic core of block copolymer micelles has been discussed intensively.[1] Here, an exchange of hydrophobic drugs into hydrophobic domains of plasma proteins happens quiet easily and especially under in vivo conditions.[58] During the uptake process of the drug, no uptake of the micelles is necessary. A close contact is sufficient to enable the diffusion of the hydrophobic entity to another hydrophobic domain.[59] According to our present knowledge the fact, whether the carrier is crosslinked or not, has, however, only a minor influence on this, [1] because the (not covalently linked) drug can diffuse freely, even in crosslinked micellar carriers. Thus, only a covalent linkage can prevent a premature release of drugs (hydrophobic entities). In this context, it is interesting that recently also reversibly crosslinkable carriers for the transport of DNA and mRNA have been prepared.[60,61]

The adsorption of complement factors and other opsonin proteins, as observed here, may, however, be significant as it can limit the circulation time and modify the body distribution.[26,62–64]

3. Conclusion

Our results show that crosslinking of the inner hydrophobic core of block copolymers is significant to reduce the formation of a protein corona compared to noncrosslinked micelles. This happens despite the low CMC of the amphiphilic block copolymers (range from 10^{-5} to 10^{-4} mg mL^{-1}[30,44,49]). The noncrosslinked polymeric micelles adsorb more proteins (47 instead of 19 types of proteins (for the crosslinked micelles)). On the other hand, the absolute amount of adsorbed proteins is—under the applied conditions—still relatively small and according to our previous results, adsorption is typically less than one protein per micelle.[17] Thus, the situation is far away from corona formation on polystyrene nanoparticles and a situation, where the surface gets covered and shielded by a hard protein corona comprising hundreds of proteins per particle. The enrichment of proteins in the nanoparticle fraction can only be detected by mass spectrometry in combination with negative controls. As many of the enriched proteins on the noncrosslinked micelles belong to the complement and coagulation cascade, noncrosslinked polymeric micelles of this type might by recognized by the immune cells and thus display reduced circulation times.

We assume that the stronger interaction of the noncrosslinked particles with plasma proteins is a result of the dynamic nature of the block copolymers. Even if their CMC is relatively low, some of the block copolymers (unimers) can leave the micelle in equilibrium. Thereafter, either the free unimers or the "modified/partly unshielded" micelle can interact with plasma proteins. As this is a general property of the dynamic system, we suppose that it happens for all noncrosslinked block copolymer micelles. We consider it reasonable that they interact thereby also with apolipoproteins, which possess hydrophobic parts and are involved in the transport of lipids.

In combination with previous work,[17] this paper demonstrates the potential of core-crosslinking to minimize interactions of polymeric micelles with plasma proteins.

4. Experimental Section

Materials: A 20-fold stock solution of the used phosphate buffered saline was prepared out of sodium chloride, potassium chloride, disodium phosphate, and potassium phosphate with a final salt concentration of 151.7 mmol L^{-1}. The stock solution was also filtrated (Millipore GHP 0.2 µm) before using it in the AF4 system.

Human blood plasma was provided from the Transfusionszentrale of the Medical Department of the Johannes Gutenberg-University Mainz. It was pooled of six healthy donors and stabilized with ethylenediaminetetraacetic acid (EDTA).

Synthesis and Preparation of Core-Crosslinked pHPMA Micelles: Analogous to the protocol of Kramer et al.,[29] core-crosslinked pHPMA micelles were prepared out of amphiphilic poly(*N*-(2-hydroxypropyl) methacrylamide)-*b*-poly(lauryl methacrylate-*ran*-hymecromone methacrylate) block copolymers by solvent switching. After obtaining the micelles the hymecromone units in the hydrophobic block were dimerized in a [2+2] photocycloaddition by UV light irradiation to provide a core-crosslinking of the micelles. The pHPMA-*b*-pLMA-*stat*-pHCMA block copolymer was synthesized via RAFT polymerization of PFPMA with 4-cyano-4-((thiobenzoyl)sulfanyl)pentaonic acid as CTA and AIBN as initiator. In a second step the pPFPMA homoblock was deployed as a macro-CTA for the polymerization of LMA and HCMA. After removing the dithiobenzoate end group the pHPMA-*b*-pLMA-*stat*-pHCMA precursor polymer was transferred with 2-hydroxyaminopropanol via aminolysis into pHPMA-*b*-pLMA-*stat*-pHCMA. Hereby, the mass ratio of each block was 80–10–10% (pHPMA to pLMA to pHCMA) and the molecular weight of the block copolymer was 16 800 g mol^{-1}.

Synthesis and Preparation of Noncrosslinked pHPMA Micelles: Analogous to the protocol of Kramer et al.,[29] noncrosslinked pHPMA micelles were prepared out of amphiphilic poly(*N*-(2-hydroxypropyl) methacrylamide)-*b*-poly(lauryl methacrylate) block copolymers by solvent switching. The pHPMA-*b*-pLMA block copolymer was synthesized via RAFT polymerization of PFPMA with 4-cyano-4-((thiobenzoyl)sulfanyl)pentaonic acid as CTA and AIBN as initiator. In a second step, the pPFPMA homoblock was deployed as a macro-CTA for the polymerization of LMA. After removing the dithiobenzoate end group the pPFPMA-*b*-pLMA precursorpolymer was transferred with 2-hydroxyaminopropanol via aminolysis into pHPMA-*b*-pLMA. Hereby, the mass ratio of each block was 80–20% (pHPMA to pLMA) and the molecular weight of the block copolymer was 17 300 g mol^{-1}.

Incubation with Human Blood Plasma: All nanoparticles (30 mg mL^{-1}) were incubated with EDTA-stabilized, pure, and undiluted plasma 1:1 v:v at 37 °C for 1 h. For a sufficient separation the AF4 is limited to a maximal plasma concentration of 5 vol%. Therefore, after incubation the samples had to be diluted with PBS to a particle concentration of 1.5 g L^{-1} and a 5 vol% solution of plasma and immediately measured in AF4.

Thus, to enable an incubation of the nanoparticles with undiluted plasma, the initial particle concentration had to be high, since the mixture had to be diluted before the AF4 measurement.

Separation by AF4: The AF4 measurements were performed using an installation from the ConSenxuS GmbH. The setup was composed of a constaMETRICR 3200 main pump and a Spectra Series UV150 detector from Thermos Separation, a Dark V3 LS Detector from ConSenxuS GmbH, a Pharmacia P-3500 injection pump, a LV-F flow controller from HORIBA ATEC, a Waters In-Line Degasser-AF, and a separation channel with a 190 µm spacer and a cellulose membrane with a molecular weight cut-off of 10 kDa, which is suitable for protein separation.[65] The UV absorption was detected at 220 nm. For all measurements, phosphate buffered saline (151.7×10^{-3} M) was used as solvent. The solvent also contained sodium azide in a concentration of 0.2×10^{-3} M. The main flow was 1 mL min^{-1} higher than the crossflow for each measurement. For each nanoparticle the crossflow is illustrated in the respective AF4 elugram. Every measurement was carried out at least three times from three independent incubation experiments. Nanoparticle fractions were collected from 12.5 to 15.8 min for the noncrosslinked pHPMA NPs and from 15 to 18.3 min for the crosslinked pHPMA NPs. To increase the concentration of the collected fractions from the AF4 after the separation process, they were filtrated with Amikon Ultra Centrifugal Filters from Merck Millipore with a regenerated cellulose membrane and a molecular weight cut off of 3 kDa. Since even the smallest plasma proteins (such as β2 microglobulin) has a molecular weight of > 10 kDa,[66] there should be no loss of proteins during the spin filtration.

SDS PAGE: The SDS-PAGE experiments were performed following the general protocol of Laemmli.[67] The polyacrylamide gels were composed of a 12%-separation gel (with 8% stacking gel) and the electrophoresis was carried out for 45 min at 200 V with a Mini-PROTEAN Tetra Vertical electrophoresis-chamber from BIO-RAD. 7.5 µL of each sample was incubated with 2.5 µL loading buffer (NuPAGE LDS Sample Buffer, Invitrogen) for 5 min at 95 °C. Novex Sharp Pre-Stained Protein Standard from INVITROGEN was loaded on each gel as a protein ladder for comparison. The proteins in the gels were visualized using a Coomassie Blue treatment and a silver staining.

DLS: For dynamic light scattering experiments of the core-crosslinked micelles the collected fractions from the AF4 were prepared in a dustfree flowbox. They were filtered with syringe filters from PALL Life Science with a diameter of 13 mm and a GHP membrane (0.2 µm pores) into dust free cylindrical scattering cells (Suprasil, 20 mm diameter). The measurements were performed with a Uniphase He/Ne Laser (632.8 nm, 22 mW), an ALV-SP125 Goniometer, an ALV/High QE APD-Avalanche photodiode, an ALV5000/E/PCI-correlator, and a Lauda RC-6 thermostat unit. All angular dependent measurements were carried out in 20° steps between 30° and 150°. Data analysis was performed according to the procedure described by Rausch et al.[68,69]

For size analysis of the noncrosslinked micelles, a Malvern Zetasizer NanoZS was used. Samples were prepared at 1 mg mL^{-1} in PBS or the collected samples from the AF4 runs were used. Each sample was independently measured five times and analyzed by its mean average and standard deviation.

Protein Digestion: Lyophilized protein corona proteins were digested according to the SP3 ("Single-Pot Solid-Phase-Enhanced Sample Preparation") protocol.[70] After solubilization in SDS-Lysis buffer (1% SDS, 1x complete Protease Inhibitor Cocktail-EDTA, 50×10^{-3} M HEPES, pH 8,5), proteins were reduced by adding 5 µL of 200×10^{-3} M Dithiothreitol (DTT) per 100 µL lysate (45 °C, 30 min). Free cysteines were subsequently alkylated by adding 10 µL 100×10^{-3} M Iodoacetamide (IAA) per 100 µL lysate (Room temperature, 30 min, in the dark). Subsequently, remaining IAA was quenched by adding 10 µL 200×10^{-3} M DTT per 100 µL lysate. Magnetic carboxylate modified particles Beads (SpeedBeads, Sigma) were used for Protein Clean-up and Acetonitrile (ACN), in a final concentration of 70%, was added to the samples to induce the binding of the proteins to the beads by hydrophilic interactions (Room temperature, 18 min). By incubating the bead-protein mixture on a magnetic stand for 2 min, the sample was bound to the magnet and the supernatant was removed, followed by two washing-steps with 70% ethanol (EtOH), addition of 180 µL ACN, incubation for 15 s and removal of the solvent. Finally, 5 µL digest buffer (50×10^{-3} M ammonium bicarbonate, 1:25 w/w trypsin:protein ratio) were added to the air-dried bead-protein mixtures and incubated over night at 37 °C. To purify peptides after digestion, ACN was added to a final concentration of 95%. After another washing step (Sielaff et al., 2017 for detailed information) the beads were resuspended in 10 µL 2% dimethyl sulfoxide (DMSO) (in water), put into an ultrasonic bath for 1 min and then shortly centrifuged. 10 µL of the resulting supernatant was mixed with 5 µL 100 fmol $µL^{-1}$ Enolase digest (Waters, Eschborn, Germany) and acidified with 5 µL 1% formic acid (FA).

LC-MS analysis: Liquid chromatography (LC) of tryptic peptides was performed on a NanoAQUITY UPLC system (Waters Corporation, Milford, MA) equipped with 75×10^{-6} M × 250 mm HSS-T3 C18 column

Macromolecular Bioscience
www.mbs-journal.de

(Waters corporation). Mobile phase A was 0.1% v/v FA, and 3% v/v DMSO in water. Mobile phase B was 0.1% v/v FA and 3% v/v DMSO in acetonitrile (ACN). Peptides were separated running a gradient from 5% to 60% v/v mobile phase B at a flow rate of 300 nL min^{-1} over 60 min. The column was heated to 55 °C. MS analysis of eluting peptides was performed by data-independent acquisition (DIA) in MS^E. In brief, precursor ion information was collected in low-energy MS mode at a constant collision energy of 4 eV. Fragment ion information was obtained in the elevated energy scan applying drift-time specific collision energies. The spectral acquisition time in each mode was 0.6 s with a 0.05 s-interscan delay resulting in an overall cycle time of 1.3 s for the acquisition of one cycle of low and elevated energy data. [Glu1]-fibrinopeptide was used as lock mass at 100 fmol μL^{-1} and sampled every 30 s into the mass spectrometer via the reference sprayer of the NanoLockSpray source. All samples were analyzed in three technical replicates.

Data Processing and Label-Free Quantification: MS^E data processing and database search was performed using ProteinLynx Global Server (PLGS, ver. 3.0.2, Waters Corporation). The resulting proteins were searched against UniProt Human proteome database (UniProtKB release 2017_05, 20 201 entries) supplemented with a list of common contaminants. The database search was specified by trypsin as enzyme for digestion and peptides with up to two missed cleavages were included. Furthermore, Carbamidomethyl cysteine was set as fixed modification and oxidized methionine as variable modification. False discovery rate assessment for peptide and protein identification was done using the target-decoy strategy by searching a reverse database and was set to 0.01 for database search in PLGS.

Retention time alignment, exact mass retention time, as well as normalization and filtering was performed in ISOQuant ver.1.8.[71,72] By using TOP3 quantification,[73] absolute in-sample amounts of proteins were calculated. Statistical analysis was done in Perseus,[74] by performing two-tailed, paired–tests, and subsequent Benjamini–Hochberg correction.[75] Q-values < 0.05 were considered as significant.

Supporting Information

Supporting Information is available from the Wiley Online Library or from the author.

Acknowledgements

The authors acknowledge support of the DFG (SFB 1066, projects A7 and B11). Furthermore, Ruben Spohrer is thanked for help with LC-MS measurements. Christine Rosenauer and Svenja Morsbach (MPI for Polymer Science) are thanked for help with dynamic light scattering measurements.

Open access funding enabled and organized by Projekt DEAL.

Conflict of Interest

The authors declare no conflict of interest.

Data Availability Statement

Data available on request from the authors.

Keywords

asymmetrical flow field-flow fractionation, core-crosslinking, polymer micelles, protein corona

Received: December 4, 2020
Revised: January 17, 2021
Published online: February 4, 2021

[1] M. Talelli, M. Barz, C. J. F. Rijcken, F. Kiessling, W. E. Hennink, T. Lammers, *Nano Today* **2015**, *10*, 93.
[2] B. Sahoo, M. Goswami, S. Nag, S. Maiti, *Chem. Phys. Lett.* **2007**, *445*, 217.
[3] R. García-Álvarez, M. Hadjidemetriou, A. Sánchez-Iglesias, L. M. Liz-Marzán, K. Kostarelos, *Nanoscale* **2018**, *10*, 1256.
[4] A. Hilla, C. K. Paynea, *RSC Adv.* **2010**, *8*, 4017.
[5] N. Bertrand, P. Grenier, M. Mahmoudi, E. M. Lima, E. A. Appel, F. Dormont, J. M. Lim, R. Karnik, R. Langer, O. C. Farokhzad, *Nat. Commun.* **2017**, *8*, 777.
[6] S. Ritz, S. Scho, N. Kotman, G. Baier, A. Musyanovych, J. Kuharev, K. Landfester, H. Schild, O. Jahn, S. Tenzer, V. Maila, *Biomacromolecules* **2015**, *16*, 1311.
[7] A. Salvati, A. S. Pitek, M. P. Monopoli, K. Prapainop, F. B. Bombelli, D. R. Hristov, P. M. Kelly, C. Åberg, E. Mahon, K. A. Dawson, *Nat. Nanotechnol.* **2013**, *8*, 137.
[8] Q. Hu, C. J. F. Rijcken, E. Van Gaal, P. Brundel, H. Kostkova, T. Etrych, B. Weber, M. Barz, F. Kiessling, J. Prakash, G. Storm, W. E. Hennink, T. Lammers, *J. Controlled Release* **2016**, *244*, 314.
[9] D. Yang, L. Yu, S. Van, *Cancers* **2011**, *3*, 17.
[10] A. Varela-Moreira, Y. Shi, M. H. A. M. Fens, T. Lammers, W. E. Hennink, R. M. Schiffelers, *Mater. Chem. Front.* **2017**, *1*, 1485.
[11] F. Atrafi, H. Dumez, R. H. J. Mathijssen, C. W. Menke, J. Costermans, C. J. F. Rijcken, R. Hanssen, F. A. L. M. Eskens, P. Schöffski, *J. Clin. Oncol.* **2019**, *37*, 3026.
[12] Q. Hu, C. J. Rijcken, R. Bansal, W. E. Hennink, G. Storm, J. Prakash, *Biomaterials* **2015**, *53*, 370.
[13] D. Klepac, S. Petrova, P. Chytil, D. A. Weitz, S. K. Filippov, *Nanoscale* **2018**, *10*, 6194.
[14] X. Wang, C. Yang, C. Wang, L. Guo, T. Zhang, Z. Zhang, H. Yan, K. Liu, *Mater. Sci. Eng. C* **2016**, *59*, 766.
[15] M. Yokoyama, M. Miyauchi, N. Yamada, T. Okano, Y. Sakurai, K. Kataoka, S. Inoue, *Cancer Res.* **1990**, *50*, 1693.
[16] J. Lu, S. C. Owen, M. S. Shoichet, *Macromolecules* **2011**, *44*, 6002.
[17] I. Alberg, S. Kramer, M. Schinnerer, Q. Hu, C. Seidl, C. Leps, N. Drude, D. Möckel, C. Rijcken, T. Lammer, M. Diken, M. Maskos, S. Morsbach, K. Landfester, S. Tenzer, M. Barz, R. Zentel, *Small* **2020**, *16*, 1907574.
[18] W. Richtering, I. Alberg, R. Zentel, *Small* **2020**, *16*, 2002162.
[19] P. Jain, R. S. Pawar, R. S. Pandey, J. Madan, S. Pawar, P. K. Lakshmi, M. S. Sudheesh, *Biotechnol. Adv.* **2017**, *35*, 889.
[20] D. Docter, U. Distler, W. Storck, J. Kuharev, D. Wünsch, A. Hahlbrock, S. K. Knauer, S. Tenzer, R. H. Stauber, *Nat. Protoc.* **2014**, *9*, 2030.
[21] S. Behzadi, V. Serpooshan, R. Sakhtianchi, B. Müller, K. Landfester, D. Crespy, M. Mahmoudi, *Colloids Surf., B* **2014**, *123*, 143.
[22] M. Lundqvist, J. Stigler, T. Cedervall, T. Berggård, M. B. Flanagan, I. Lynch, G. Elia, K. Dawson, *ACS Nano* **2011**, *5*, 7503.
[23] K. Obst, G. Yealland, B. Balzus, E. Miceli, M. Dimde, C. Weise, M. Eravci, R. Bodmeier, R. Haag, M. Calderón, N. Charbaji, S. Hedtrich, *Biomacromolecules* **2017**, *18*, 1762.
[24] M. Hadjidemetriou, S. McAdam, G. Garner, C. Thackeray, D. Knight, D. Smith, Z. Al-ahmady, M. Mazza, J. Rogan, A. Clamp, K. Kostarelos, *Adv. Mater.* **2019**, *31*, 1803335.
[25] M. Mahmoudi, N. Bertrand, H. Zope, O. C. Farokhzad, *Nano Today* **2016**, *11*, 817.
[26] D. Pozzi, G. Caracciolo, A. L. Capriotti, C. Cavaliere, S. Piovesana, V. Colapicchioni, S. Palchetti, A. Riccioli, A. Lagana, *Mol. BioSyst.* **2014**, 2815.

[27] A. P. Ault, D. I. Stark, J. L. Axson, J. N. Keeney, A. D. Maynard, I. L. Bergin, M. A. Philbert, *Environ. Sci. Nano* **2016**, *3*, 1510.
[28] V. Mirshafiee, M. Mahmoudi, K. Lou, J. Cheng, M. L. Kraft, *Chem. Commun.* **2013**, *49*, 2557.
[29] S. Kramer, K. O. Kim, R. Zentel, *Macromol. Chem. Phys.* **2017**, *218*, 1700113.
[30] M. Allmeroth, D. Moderegger, D. Gündel, H. Buchholz, N. Mohr, K. Koynov, F. Rösch, O. Thews, R. Zentel, *J. Controlled Release* **2013**, *172*, 77.
[31] M. Elsabahy, S. Samarajeewa, J. E. Raymond, C. Clark, K. L. Wooley, *J. Mater. Chem. B* **2013**, *1*, 5241.
[32] V. Hong Nguyen, B.-J. Lee, *Int. J. Nanomed.* **2017**, *12*, 3137.
[33] S. Schöttler, K. Landfester, V. Mailänder, *Angew. Chem., Int. Ed.* **2016**, *55*, 8806.
[34] E. Ostuni, R. G. Chapman, R. E. Holmlin, S. Takayama, G. M. Whitesides, *Langmuir* **2001**, *17*, 5605.
[35] M. Kokkinopoulou, J. Simon, K. Landfester, V. Mailänder, I. Lieberwirth, *Nanoscale* **2017**, *9*, 8858.
[36] J. Simon, T. Wolf, K. Klein, K. Landfester, F. R. Wurm, V. Mailänder, *Angew Chem. Int. Ed. Engl.* **2018**, *57*, 5548.
[37] S. Schöttler, G. Becker, S. Winzen, T. Steinbach, K. Mohr, K. Landfester, V. Mailänder, F. R. Wurm, *Nat. Nanotechnol.* **2016**, *11*, 372.
[38] V. P. Zhdanov, *Curr. Opin. Colloid Interface Sci.* **2019**, *41*, 95.
[39] C. M. Lo Giudice, L. M. Herda, E. Polo, K. A. Dawson, *Nat. Commun.* **2016**, *7*, 13475.
[40] J. Wang, U. B. Jensen, G. V. Jensen, S. Shipovskov, V. S. Balakrishnan, D. Otzen, J. S. Pedersen, F. Besenbacher, D. S. Sutherland, *Nano Lett.* **2011**, *11*, 4985.
[41] T. Miclăuş, C. Beer, J. Chevallier, C. Scavenius, V. E. Bochenkov, J. J. Enghild, D. S. Sutherland, *Nat. Commun.* **2016**, *7*, 11770.
[42] M. Allmeroth, D. Moderegger, B. Biesalski, K. Koynov, F. Rösch, O. Thews, R. Zentel, *Biomacromolecules* **2011**, *12*, 2841.
[43] Y. Shi, T. Lammers, G. Storm, W. E. Hennink, *Macromol. Biosci.* **2017**, *17*, 1600160.
[44] L. Nuhn, M. Barz, R. Zentel, *Macromol. Biosci.* **2014**, *14*, 607.
[45] P. A. Vasey, S. B. Kaye, R. Morrison, C. Twelves, P. Wilson, R. Duncan, A. H. Thomson, L. S. Murray, T. E. Hilditch, T. Murray, S. Burtles, D. Fraier, E. Frigerio, J. Cassidy, *Clin. Cancer Res.* **1999**, *5*, 83.
[46] P. Chytil, E. Koziolová, T. Etrych, K. Ulbrich, *Macromol. Biosci.* **2018**, *18*, 1700209.
[47] M. Barz, F. K. Wolf, F. Canal, K. Koynov, M. J. Vicent, H. Frey, R. Zentel, *Macromol. Rapid Commun.* **2010**, *31*, 1492.
[48] J. Kopeček, P. Kopečková, *Adv. Drug Delivery Rev.* **2010**, *62*, 122.
[49] M. Barz, R. Luxenhofer, R. Zentel, A. V. Kabanov, *Biomaterials* **2009**, *30*, 5682.
[50] S. Kramer, J. Langhanki, M. Krumb, T. Opatz, M. Bros, R. Zentel, *Macromol. Biosci.* **2019**, *19*, 1800481.
[51] T. Lammers, R. Kühnlein, M. Kissel, V. Subr, T. Etrych, R. Pola, M. Pechar, K. Ulbrich, G. Storm, P. Huber, P. Peschke, *J. Controlled Release* **2005**, *110*, 103.
[52] C. Zhao, L. Li, J. Zheng, *Langmuir* **2010**, *26*, 17375.
[53] J. C. Giddings, *Sep. Sci.* **1966**, *1*, 123.
[54] T. J. Cho, V. A. Hackley, *Anal. Bioanal. Chem.* **2010**, *398*, 2003.
[55] F. A. Messaud, R. D. Sanderson, J. R. Runyon, T. Otte, H. Pasch, S. K. R. Williams, *Prog. Polym. Sci.* **2009**, *34*, 351.
[56] S. Podzimek, *Light Scattering, Size Exclusion Chromatography and Asymmetric Flow Field Flow Fractionation*, John Wiley & Sons, Inc., NJ **2011**.
[57] M. Wagner, S. Holzschuh, A. Traeger, A. Fahr, U. S. Schubert, *Anal. Chem.* **2014**, *86*, 5201.
[58] Y. Li, M. S. Budamagunta, J. Luo, W. Xiao, J. C. Voss, K. S. Lam, *ACS Nano* **2012**, *6*, 9485.
[59] S. Tomcin, A. Kelsch, R. H. Staff, K. Landfester, R. Zentel, V. Mailänder, *Acta Biomater.* **2016**, *35*, 12.
[60] P. Heller, D. Hobernik, U. Lächelt, M. Schinnerer, B. Weber, M. Schmidt, E. Wagner, M. Bros, M. Barz, *J. Controlled Release* **2017**, *258*, 146.
[61] N. Ritt, S. Berger, E. Wagner, R. Zentel, *A C S Appl. Polym. Mater.* **2020**, *2*, 5469.
[62] H. Gao, Q. He, *Expert Opin. Drug Delivery* **2014**, *11*, 409.
[63] T. M. Goppert, R. H. Müller, *Pharm. Nanotechnol.* **2005**, *302*, 172.
[64] P. Camner, M. Lundborg, L. Låstbom, P. Gerde, N. Gross, C. Jarstrand, *J. Appl. Physiol.* **2002**, *92*, 2608.
[65] M. Marioli, W. T. Kok, *Anal. Bioanal. Chem.* **2019**, *411*, 2327.
[66] J. Tattersall, *Contrib. Nephrol.* **2007**, *158*, 201.
[67] U. K. Laemmli, *Nature* **1970**, *227*, 680.
[68] K. Mohr, M. Sommer, G. Baier, S. Schöttler, P. Okwieka, S. Tenzer, K. Landfester, V. Mailänder, M. Schmidt, R. G. Meyer, *Nanomed. Nanotechnol.* **2014**, *5*, 1000193.
[69] K. Rausch, A. Reuter, K. Fischer, M. Schmidt, *Biomacromolecules* **2010**, *11*, 2836.
[70] M. Sielaff, J. Kuharev, T. Bohn, J. Hahlbrock, T. Bopp, S. Tenzer, U. Distler, *J. Proteome Res.* **2017**, *16*, 4060.
[71] U. Distler, J. Kuharev, P. Navarro, S. Tenzer, *Nat. Protoc.* **2016**, *11*, 795.
[72] U. Distler, J. Kuharev, P. Navarro, Y. Levin, H. Schild, S. Tenzer, *Nat. Methods* **2014**, *11*, 167.
[73] J. C. Silva, M. V. Gorenstein, G.-Z. Li, J. P. C. Vissers, S. J. Geromanos, *Mol. Cell. Proteomics* **2006**, *5*, 144.
[74] S. Tyanova, J. Cox, *Methods Mol. Biol.* **2018**, *1711*, 133.
[75] Y. Benjamini, Y. Hochberg, *J. R. Statist.. Soc. B* **1995**, *57*, 289.